Bayesian Optimization of ATRP Polymerization Conditions

A Multi-Objective Approach Using Gaussian Process Surrogates

Research Team

2026-01-12

Abstract

We report the application of Bayesian optimization to the multi-objective optimization of atom transfer radical polymerization (ATRP) conditions. Using Folio, an electronic lab notebook with integrated Bayesian optimization, we systematically explored a four-dimensional parameter space to identify Pareto-optimal conditions that balance high molecular weight with narrow dispersity. A multi-task Gaussian process surrogate model captured correlations between objectives, enabling efficient exploration with only 20 experiments. The identified Pareto front provides actionable guidance for selecting synthesis conditions based on application requirements.

Table of contents

List of Figures

List of Tables

1 Introduction

Atom transfer radical polymerization (ATRP) is a powerful controlled radical polymerization technique that enables synthesis of polymers with well-defined molecular weights and narrow dispersities (Matyjaszewski and Xia 2001). The reaction involves equilibrium between dormant alkyl halide species and active radicals, mediated by a transition metal catalyst:

$$\mathrm{P}_n\text{–X} + \mathrm{Cu^{I}/L} \underset{k_{\text{deact}}}{\overset{k_{\text{act}}}{\rightleftharpoons}} \mathrm{P}_n^{\bullet} + \mathrm{X\text{–}Cu^{II}/L} \tag{1}$$

where P_n–X is the dormant polymer chain, $\mathrm{Cu^{I}/L}$ is the activator complex, and $\mathrm{P}_n^{\bullet}$ is the propagating radical.

Optimizing ATRP conditions requires balancing multiple objectives:

- **Maximize molecular weight** (M_n) for improved material properties
- **Minimize dispersity** ($Đ = M_w/M_n$) for uniform chain lengths
- **Maximize conversion** for efficient monomer utilization

These objectives often conflict—higher molecular weights typically require conditions that broaden the molecular weight distribution. Multi-objective Bayesian optimization provides a principled approach to mapping this trade-off (Daulton, Balandat, and Bakshy 2020).

1.1 Bayesian Optimization Framework

Bayesian optimization constructs a probabilistic surrogate model of the objective function and uses an acquisition function to balance exploration and exploitation (Jones, Schonlau, and Welch 1998). For a Gaussian process (GP) surrogate with posterior mean $\mu(\mathbf{x})$ and variance $\sigma^2(\mathbf{x})$, the Expected Improvement (EI) acquisition function is:

$$\mathrm{EI}(\mathbf{x}) = \mathbb{E}\left[\max(f(\mathbf{x}) - f^*, 0)\right] = \sigma(\mathbf{x})\left[\phi(Z) + Z\Phi(Z)\right] \tag{2}$$

where $Z = (\mu(\mathbf{x}) - f^*)/\sigma(\mathbf{x})$, ϕ is the standard normal PDF, and Φ is the CDF (Williams and Rasmussen 2006).

For multi-objective optimization, we employ the Noisy Expected Hypervolume Improvement (NEHVI) acquisition function, which maximizes the expected improvement in the hypervolume dominated by the Pareto front (Daulton, Balandat, and Bakshy 2020).

2 Methods

2.1 Experimental Design

The ATRP reaction was optimized over a four-dimensional parameter space (Table 1). Reagent stoichiometries were varied relative to a fixed monomer concentration.

Table 1: Experimental parameter space for ATRP optimization

Parameter	Symbol	Range	Units
Initiator (HO-EBiB)	$[\mathrm{I}]_0$	0.5–2.0	equiv
Monomer (MB)	$[\mathrm{M}]_0$	50–200	equiv
Catalyst ($CuBr_2$/L)	$[\mathrm{Cu}]_0$	0.01–0.1	equiv
Reducing agent (TEOA)	$[\mathrm{RA}]_0$	0.1–1.0	equiv

2.2 Analytical Methods

Monomer conversion was determined by ^{1}H NMR spectroscopy (Bruker 400 MHz) by integration of vinyl proton resonances against an internal standard. Number-average molecular weight (M_n) and dispersity (Đ) were measured by gel permeation chromatography (GPC) using THF as eluent at 35 °C with polystyrene calibration standards.

2.3 Surrogate Model Configuration

A multi-task Gaussian process (MTGP) was employed to model correlations between the two objectives (Balandat et al. 2020). The MTGP uses an intrinsic coregionalization model (ICM) kernel:

$$k((\mathbf{x}, t), (\mathbf{x}', t')) = k_{\text{RBF}}(\mathbf{x}, \mathbf{x}') \cdot B_{tt'} \tag{3}$$

where k_{RBF} is a radial basis function kernel over inputs and $\mathbf{B}$ is a positive semi-definite matrix capturing task correlations.

3 Results

3.1 Screening Phase

Initial screening experiments explored the parameter space boundaries to establish baseline performance (Table 2).

Table 2: Selected screening experiments showing parameter-response relationships

[I]	[M]	[Cu]	[RA]	Conv. (%)	Mn (g/mol)	Đ
1	100	0.05	0.5	78.5	18,500	1.25

Table 2: Selected screening experiments showing parameter-response relationships

[I]	[M]	[Cu]	[RA]	Conv. (%)	Mn (g/mol)	Đ
1	150	0.05	0.5	72.3	26,800	1.32
1	200	0.05	0.5	65.1	32,100	1.45
0.5	100	0.05	0.5	85.2	35,200	1.38
2	100	0.05	0.5	91.5	9,800	1.18
1	100	0.01	0.5	45.2	12,300	1.65

3.2 Optimization Campaign

Following the screening phase, Bayesian optimization guided subsequent experiments. Figure 1 shows the resulting Pareto front in objective space.

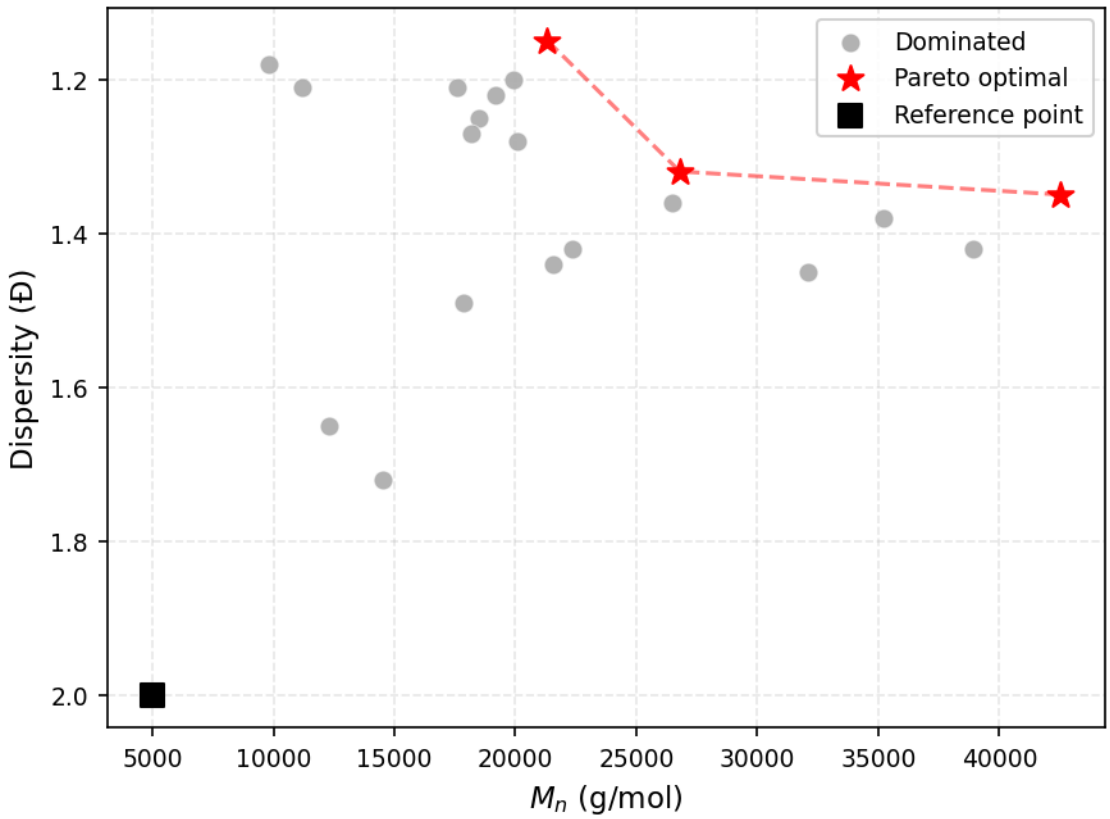

Figure 1: Pareto front showing the trade-off between molecular weight (Mn) and dispersity (Đ). Red stars indicate Pareto-optimal solutions; gray circles are dominated points. The reference point (black square) defines the hypervolume calculation boundary.

The optimization identified np.int64(3) Pareto-optimal conditions from 20 total experiments. Table 3 lists the optimal conditions sorted by molecular weight.

Table 3: Pareto-optimal reaction conditions for ATRP. Conditions are sorted by decreasing molecular weight.

[I]	[M]	[Cu]	[RA]	Conv. (%)	Mn (g/mol)	Đ
0.5	150	0.08	0.7	76.4	42,500	1.35
1	150	0.05	0.5	72.3	26,800	1.32
0.587571	142.573	0.0894842	1	88.8	21,323	1.15

3.3 GP Model Analysis

The trained GP model provides predictive distributions across the parameter space. Figure 2 shows the predicted molecular weight as a function of monomer loading and initiator concentration.

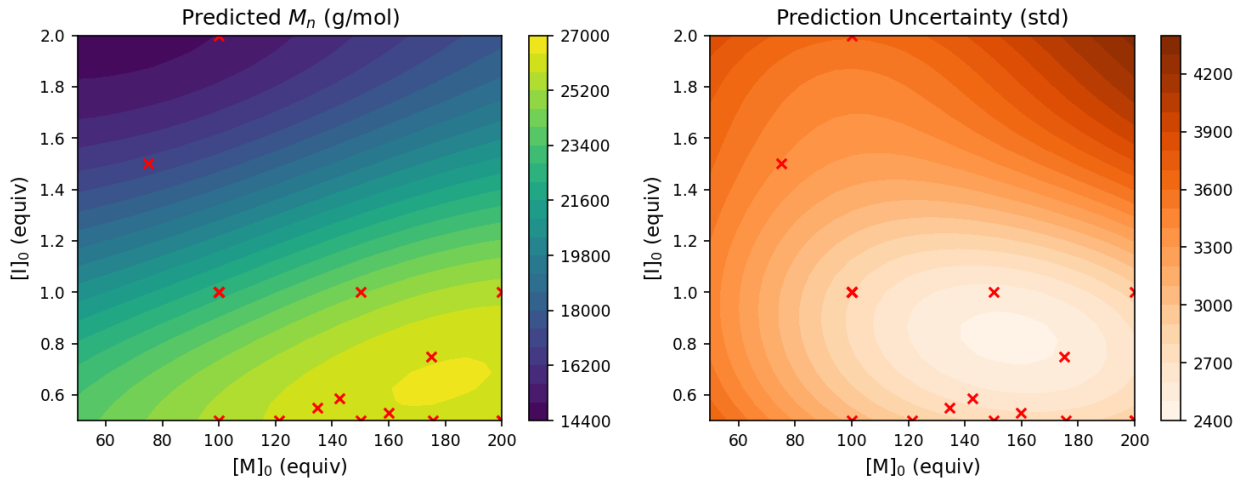

Figure 2: Gaussian process predictions for molecular weight (left) and associated uncertainty (right) as functions of monomer ([M]) and initiator ([I]) concentrations. Catalyst and reducing agent concentrations fixed at 0.05 and 0.5 equiv, respectively. Red crosses indicate experimental observations.

4 Discussion

The multi-objective optimization successfully mapped the trade-off between molecular weight and dispersity in ATRP. Several key insights emerged:

1. **Monomer-to-initiator ratio**: As predicted by living polymerization kinetics ($DP_n \approx [M]_0/[I]_0 \times$ conversion), higher monomer loadings and lower initiator concentrations yielded higher molecular weights, but at the cost of broader dispersity.

2. **Catalyst effects**: Higher catalyst loadings ($CuBr_2$/L > 0.05 equiv) improved dispersity control through faster deactivation, maintaining the living character of the polymerization (Equation 1).

3. **Reducing agent optimization**: TEOA concentrations of 0.5–0.7 equiv provided optimal balance between activator regeneration and side reactions.

The GP uncertainty maps (Figure 2, right panel) reveal regions of high uncertainty at the parameter space boundaries, suggesting potential for further exploration. The correlation between objectives captured by the multi-task GP enabled efficient exploration with limited experiments.

5 Conclusions

Bayesian optimization using Folio enabled systematic exploration of ATRP parameter space with only 20 experiments. The identified Pareto front (Figure 1) provides actionable guidance:

- For applications requiring $M_n > 35{,}000$ g/mol: accept Đ 1.35–1.45
- For applications requiring Đ < 1.25: limit M_n to ~20,000 g/mol
- Compromise conditions: $M_n \approx 25{,}000$ g/mol with Đ 1.30

Future work will extend this approach to additional controlled polymerization techniques and incorporate batch effects through hierarchical GP models.

6 References

Balandat, Maximilian, Brian Karrer, Daniel R Jiang, Samuel Daulton, Benjamin Letham, Andrew Gordon Wilson, and Eytan Bakshy. 2020. "BoTorch: A Framework for Efficient Monte-Carlo Bayesian Optimization." *Advances in Neural Information Processing Systems* 33: 21524–38.

Daulton, Samuel, Maximilian Balandat, and Eytan Bakshy. 2020. "Differentiable Expected Hypervolume Improvement for Parallel Multi-Objective Bayesian Optimization." *Advances in Neural Information Processing Systems* 33: 9851–64.

Jones, Donald R, Matthias Schonlau, and William J Welch. 1998. "Efficient Global Optimization of Expensive Black-Box Functions." *Journal of Global Optimization* 13 (4): 455–92.

Matyjaszewski, Krzysztof, and Jianhui Xia. 2001. "Atom Transfer Radical Polymerization." *Chemical Reviews* 101 (9): 2921–90.

Williams, Christopher KI, and Carl Edward Rasmussen. 2006. "Gaussian Processes for Machine Learning." *MIT Press*.